

## Redispersible Pickering emulsion powder stabilized by nanocrystalline cellulose combining with cellulosic derivatives



Jin Xie<sup>a,1</sup>, Yijing Luo<sup>a,1</sup>, Yingchong Chen<sup>a</sup>, Yang Liu<sup>a</sup>, Yueqin Ma<sup>a,b</sup>, Qin Zheng<sup>a</sup>, Pengfei Yue<sup>a,\*</sup>, Ming Yang<sup>a</sup>

<sup>a</sup> Jiangxi University of Traditional Chinese Medicine, 818 Meilingdadao Road, Nanchang 330004, China

<sup>b</sup> Department of Pharmaceutics, 908th Hospital of People's Liberation Army, Nanchang, China

### ARTICLE INFO

#### Keywords:

Cellulose nanocrystals  
Redispersible Pickering emulsions  
Carboxymethyl cellulose sodium  
Hydroxypropyl methylcellulose  
Homogenization

### ABSTRACT

The objective of this study is to use cellulose nanocrystals (CNC) combining with carboxymethyl cellulose sodium (CMC-Na) and hydroxypropyl methylcellulose (HPMC) as stabilizer to prepare novel redispersible camellia oil Pickering emulsions powder (CO-PEP). Cellulose nanocrystals modified with carboxymethyl cellulose sodium (CNCC) was prepared by homogenization technology. CNCC seemed to be rod-like particles with mean particle size of  $124.2 \pm 2.5$  nm. And the cellulose structure, crystal state and thermal property of CNCC remained unchanged during the homogenization. The combination of CNC and CMC-Na in CNCC might be dependent of physical interaction. The mean particle size of optimum CO-PEP/0.25%CNCC was  $0.569 \pm 0.023$   $\mu$ m. The CNCC based particle stabilizer might form the distinctive barrier layer around oil droplet. The redispersibility results demonstrated that 50% HPMC based CO-PEP formed large composite particle with high drug loading ability and exhibited superior redispersibility. Novel redispersible powdered Pickering emulsions could be prepared by cellulose nanocrystals combining with water-soluble cellulosic derivatives.

### 1. Introduction

Emulsion was thought to be effective strategy for encapsulation of oil (Mao, Roos, Biliaderis, & Miao, 2017). Classical emulsions are heterogeneous systems consisting of droplets of a liquid dispersed in another non-miscible or partly miscible liquid, and stabilized by surfactants or surface-active polymers or natural polymers such as proteins and polysaccharides. However, oil/water emulsions are physical instability due to degradation and oxidation of oil, microbial growth, and not facilitated for transportation. One effective way to circumvent such disadvantages was able to convert a liquid emulsion into a dry emulsions powder by mean of spray-drying (Asensio et al., 2017; Basha, Salama, & El Awdan, 2017). Moreover, a free-flowing dry emulsions powder that can be readily incorporated into all kinds of formulations. Unfortunately that, disruption of emulsion droplets and oil leakage usually occurred during dehydration of emulsions. In order to prevent coalescence of the emulsion droplets and oil leakage, hydrophilic wall materials, such as lactose, glucose, inulin, maltodextrin and hydroxypropyl methylcellulose (HPMC), can be added into the formulations prior to drying (Christensen, Pedersen, & Kristensen, 2001; Da Costa

et al., 2013; Fernandes, Borges, & Botrel, 2014; Goula & Adamopoulos, 2008).

Pickering emulsions are a new type of emulsions stabilized by solid particles instead of conventional surfactants (Berton-Carabin & Schroën, 2015; Marto, Ascenso, Simoes, Almeida, & Ribeiro, 2016). The high resistance to coalescence is a major benefit of the stabilization by solid particles requiring an interfacial solid material (Yang et al., 2017). And the solid particle should be partially wet by both liquid phases and should be weakly flocculated (Wu & Ma, 2016; Yang, Bakaic, Hoare, & Cranston, 2013). There has been increasing interest in renew-able, environment-friendly biomaterials in last recent years, and it attracts a great potential to introduce these materials into production of solid particles to stabilize Pickering emulsions. Cellulose nanocrystals (CNC) is generally regarded as ideal biomaterial due to their particularly properties, such as low density, low carbon footprint, chemical tenability, environmental sustainability, and anticipated low cost (Fujisawa, Togawa, & Kuroda, 2017). It is of particular interest for various applications such as cosmetics, pharmaceuticals, or medical implants (Sunasee, Hemraz, & Ckless, 2016). The use of CNC as stabilizer of Pickering emulsions is expected to be advantageous over some

\* Corresponding author.

E-mail address: [feigleyue@outlook.com](mailto:feigleyue@outlook.com) (P. Yue).

<sup>1</sup> Jin Xie and Yijing Luo contributed to the work equally as joint first authors.

inorganic nanoparticles when the above advantages are considered (Li et al., 2018; Wen, Yuan, Liang, & Vriesekoop, 2014; Zhou et al., 2018). CNC was conventionally produced via the acid-catalyzed hydrolysis of the cellulosic feed stock (Habibi, Lucia, & Rojas, 2010; Wen et al., 2014). The cellulosic pulp or cotton linters can be usually used as raw materials for preparing CNC (George & Sabapathi, 2015). Microcrystalline cellulose (MCC) has also recently attracted interest as a valid intermediate material for producing CNC via microfluidization method (Buffiere et al., 2017). But with decrease of particle size of CNC at process of homogenization, the surface energy of CNC was remarkably increased, and nanosized CNC particles could easily generate flocculation, aggregation or crystal growth to decrease their free energy (Wang, Zheng, Zhang, Wang, & Zhang, 2013). Polymers are known to enhance stability of nanocrystals particles by steric barrier effect (Zhen et al., 2016; Hu, Marway, Kasem, Pelton, & Cranston, 2016). Therefore, co-processed modification and combination of CNC particles with water-soluble polymers has also recently gained increasingly interest for successful production of colloidal formulation (Bandera et al., 2014; Natterodt, Sapkota, Foster, & Weder, 2017; Hu, Patten, Pelton, & Cranston, 2015). The novel aspect of the current work was CNC modified with water-soluble cellulosic derivative carboxymethyl cellulose sodium (CMC-Na) could be produced by nanocrystals-technology, and used to maintain the stability of Pickering emulsion droplets and enhance the redispersibility of dried Pickering emulsions powder.

As illustrated in Fig. 1, using camellia oil (CO) as oil phase in this study, a novel spray-dried Pickering emulsions-based powder was designed, using CNC as particle stabilizer. The objectives of this manuscript were as follows: (1) Cellulose nanocrystals modified with carboxymethyl cellulose sodium (CNCC) was prepared by means of homogenization technology. The particle size, morphology and crystals state of pretreated CNCC was evaluated. (2) CO Pickering emulsions (CO-PE/CNCC) stabilized by CNCC were prepared by homogenization technology and further converted into spray-dried CO Pickering emulsion powder (CO-PEP/CNCC) using different carbohydrate polymers as matrix formers, respectively. The particles size, morphology and redispersibility of CO-PEP/CNCC were characterized. And the solid state

and morphology of CO-PEP/CNCC was further investigated.

## 2. Materials and methods

### 2.1. Materials

Microcrystalline cellulose (MCC, mean particle size of about 50  $\mu\text{m}$ ), trehalose, maltodextrin and hydroxypropyl methylcellulose (HPMC) was commercially obtained from Fengli Jingqiu Pharmaceutical Co., Ltd. (Beijing, China). Carboxymethyl cellulose sodium (CMC-Na) was purchased from Chineway Pharmaceutical Co., Ltd. Lactose and arabic gum was kindly supplied by Anhui Sunhere Pharmaceutical Excipients Co., Ltd (Anhui, China). CO was kindly supplied by Jian Tian Yuan Medical Oil Refinery (Jiangxi, China). Inulin was purchased from Wuxi Microbio Engineering Co., Ltd. (Wuxi, China).

### 2.2. Preparation of CNCC

Cellulose nanocrystals modified with carboxymethyl cellulose sodium (CNCC)

were prepared via homogenization method. Briefly, different amount of MCC with CMC-Na were dispersed in the 100 ml water at 1000 rpm for 30 min. The gained coarse suspension composed of MCC and CMC-Na was homogenized at high pressure using a piston-gap high pressure homogenizer (AH-1000D, ATS Engineering Inc., Seeker, Canada). Firstly, 30 cycles at 200 bar, 20 cycles 500 bar were conducted as pre-milling step, and afterwards, 30 cycles at 800 bar were run to obtain the CNCC suspensions. For follow-up characterization, the CNCC nanosuspensions was further subjected to spray-drying (inlet temperature was set as 120  $^{\circ}\text{C}$ ; aspiration rate, 55%; and atomizing air flow, 50 mmHg). The dried CNCC were separated from the drying air in the cyclone (60  $^{\circ}\text{C}$  outlet temperature) and deposited at the bottom of the collector.

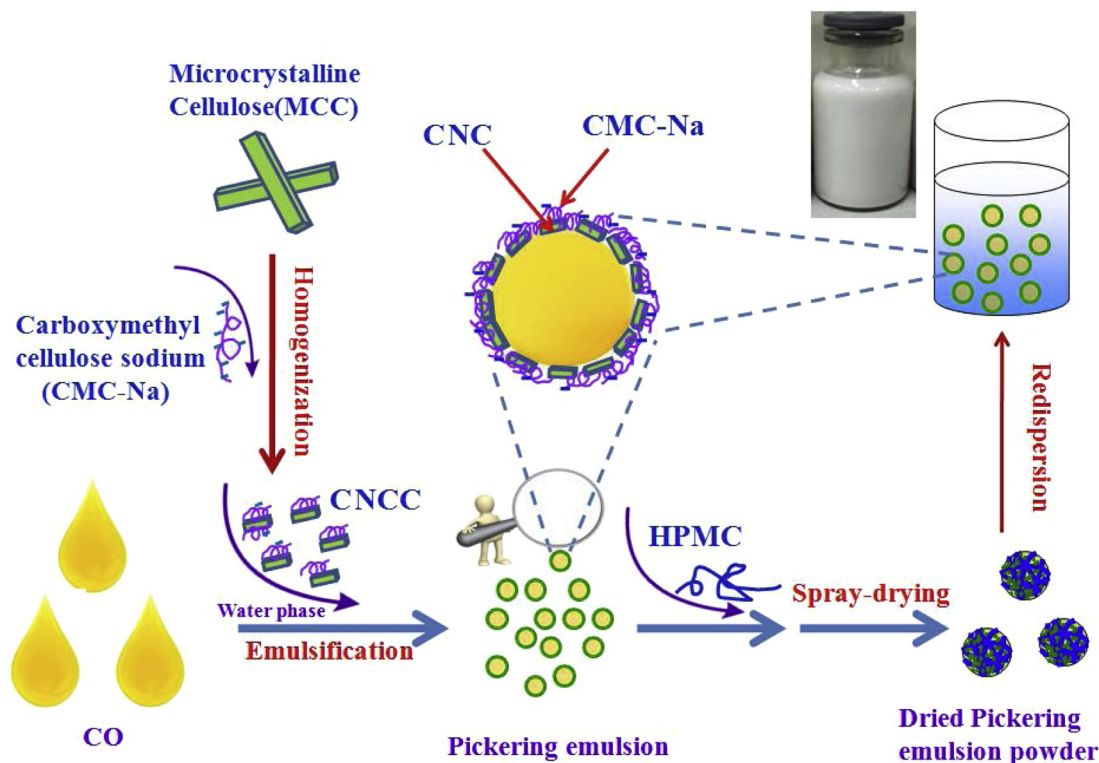


Fig. 1. Schematic illustrations of Pickering emulsion stabilized by cellulose nanocrystals combining with water-soluble cellulosic derivatives.

### 2.3. Preparation of CO Pickering emulsions (CO-PE)

CO Pickering emulsions were prepared by ultrasonic dispersion method. In briefly, different amounts of CNCC powder (10, 25 and 50 mg) were added to 9 ml deionized water respectively and redispersed into CNCC suspensions. The CNCC suspensions were used as water phase. 1 ml camellia oil (CO) was used as oil phase. The coarse CO Pickering emulsions (CO-PE) were prepared using an oil/water ratio of 1/9 (Kalashnikova, Bizot, Cathala, & Capron, 2011), and sonicated at 0.4 kW power level (3 s sonication, 2 s standby) for 1 min via a ultrasonic homogenizer (Scientz® JY96-IIN, Ningbo, China). And then the coarse CO-PE was homogenized at high pressure using a piston-gap high pressure homogenizer (AH-1000D, ATS Engineering Inc., Seeker, Canada). Firstly, 30 cycles at 200 bar, 30 cycles 500 bar were conducted as pre-milling step, and afterwards, 30 cycles at 1000 bar were applied to obtain the fine CO-PE.

### 2.4. Conversion CO-PE into CO-PEP via spray-drying

The CO-PEP was obtained by spraying the CO-PE through the nozzle of a Buchi mini spray dryer (model B290; Buchi Laboratories-Technik AG, Flawil, Switzerland). Prior to spray-drying, different concentrations of CNCC, CMC-Na, HPMC, arabic gum, trehalose, lactose, inulin and maltodextrin (relative weight of oil phase, w/w) as matrix formers was dissolved into the CO-PE, respectively. After then, the treated CO-PE was subjected to spray-drying with process parameters as follows: inlet temperature was set as 120 °C; aspiration rate, 55%; and atomizing air flow, 50 mmHg. The CO-PEP particles were separated from the drying air in the cyclone (65 °C outlet temperature) and deposited at the bottom of the collector. They were collected and kept at room temperature for future testing and evaluation.

### 2.5. Characterization of CNCC, CO-PE and CO-PEP

#### 2.5.1. Particle size and zeta potential measurements of CNCC and CO-PE

The particles size determination of CNCC suspensions and CO-PE was performed on a Mastersizer Micro Plus (Malvern Instruments Limited, Worcestershire, UK). Analysis of the diffraction patterns was done using the Mie model (“standard” presentation: dispersant refractive index = 1.33, real particle refractive index = 1.53, imaginary particle refractive index = 0.1). D10, D50 and D90 are the volumetric diameters where the 10%, 50% and 90% of the population lies below each value, respectively. All measurements were performed in triplicate. Differences of particle size of different CNCC were considered statistically significant if the p-value was less than 0.05.

The Zeta potential of CNCC suspensions and CO-PE was determined by the dynamic light scattering (Nano ZS, Malvern instrument). The samples were firstly diluted to a concentration of approximately 0.05% (w/w) using deionized water in order to avoid multiple scattering effects. All measurements were performed in triplicate. The Zeta potential was recorded as the average and standard deviation of measurements.

#### 2.5.2. Solid state of CNCC

The crystal state of the coarse MCC, CMC-Na, mixture of MCC and CMC-Na, as well as CNCC was analyzed using PXRD (PANalytical, Westborough, MA, USA), respectively. The samples were scanned for 2θ ranging from 5° to 60° at a scan rate of 0.2 °C/min. Measurements were performed at a voltage of 40 kV and 25 mA.

#### 2.5.3. Fourier transfer-infrared (FT-IR) spectroscopy of CNCC

Fourier transform infrared spectrophotometry (FT-IR Spectrometer, BRUKER IFS-55, Switzerland) was used to determine the interaction between CNCC and CMC-Na. The IR spectra of MCC, CMC-Na, the mixture of MCC and CMC-Na, and CNCC were assayed by the KBr method, respectively.

#### 2.5.4. Thermal analysis of CNCC

Thermal stabilities of the coarse MCC, CMC-Na, the mixture of MCC and CMC-Na, and CNCC were respectively determined by means of thermogravimetric analysis (TGA). 6–7 mg powder sample was weighed before being placed in a sealed perforated aluminum pan and heated from 25 °C to 500 °C at a flow rate of 10 °C·min<sup>-1</sup>. The applied nitrogen atmosphere was at a flow rate of 30 mL·min<sup>-1</sup>.

The peak melting temperature of MCC and CNCC was further evaluated by an analyzer DSC (Diamond DSC, Perkin-Elmer, USA). 6–7 mg powder sample was weighed before being placed in a sealed perforated aluminum pan and were heated from 25 °C to 300 °C at a rate of 10 °C·min<sup>-1</sup>. Nitrogen was used as the purge gas and protective gas at a flow rate of 30 ml·min<sup>-1</sup> and 150 ml·min<sup>-1</sup>, respectively.

#### 2.5.5. Morphology of CNCC, CO-PE and CO-PEP

The morphology of the comprehensive CNCC suspensions and CO-PE were analyzed by transmission electron microscopy (TEM) (JEM-1200EX; JEOL, Tokyo, Japan). The samples were diluted in distilled water and placed on a copper grid. The grid was dried at room temperature and was evaluated with the electron microscope.

Morphology of the dried CO-PEP was evaluated using scanning electron microscope (SEM) (Hitachi X650, Tokyo, Japan). The samples were glued and solidified on metal sample plates by means of carbon double-sided tape. All the samples were gold coated (thickness ≈ 15–20 nm) by means of a sputter coater (Fison Instruments, UK). The electrical potential was set as 2.0 kV at 25 mA for 10 min.

#### 2.5.6. Redispersibility of the dried CO-PEP

As previous described method (Dollo et al., 2013), 100 mg CO-PEP powders were dispersed in 10 ml distilled water by hand-shaking (5 s), and then the emulsion was shaken for 3 min operating at 250 strokes·min<sup>-1</sup> and samples were withdrawn for droplet size determination. The redispersibility index (RDI) of CO-PEP was calculated by the following equation (Ma et al., 2018).

$$RDI = \frac{D}{D_0}$$

Where  $D_0$  is the volume-weighted ( $D_{50}$ ) particle size of the freshly prepared CO-PE directly prior to spray-drying and  $D$  is the corresponding value of redispersed suspensions from CO-PEP post spray-drying. An RDI of near 1 indicated that CO-PEP can completely recover back to the original Pickering emulsions after rehydration. An RDI of more than 1.5 meant that CO-PEP can not reconstitute into the original Pickering emulsions.

## 3. Results and discussion

### 3.1. Preparation and characterization of CNCC

The particle size of freshly prepared CNCC modified with different ratios of CMC-Na was showed in Table 1. The results showed that the mean particle size of CNC (N1) without modification of CMC-Na in water was  $619.51 \pm 15.21$  nm. But the original MCC usually appeared irregular rod particles with a particle size of  $45.82 \pm 0.31$  μm (Liu et al., 2018). It was concluded that MCC could be disintegrated to nanosized crystalline cellulose via high pressure homogenization. But the mean particle size of the redispersed CNC particles without CMC-Na after spray-drying was  $1319.51 \pm 24.16$ , which meant that CNC could generate some large aggregation during spray-drying. To further enhance stability of CNC during spray-drying, the water-soluble polymer CMC-Na was introduced into production of CNCC. The mean particle size of CNCC (N2N6) modified with different ratios of CMC-Na was shown in Table 1. As the increased ratio of CMC-Na, the mean particle size of CNCC gradually decreased. The results indicated that CNCC could be disintegrated much smaller nanocrystals particles at the presence of CMC-Na, compared with that those of CNC without CMC-Na

**Table 1**  
Mean particle size of CNCC modified with different ratios of CMC-Na.

Ratio of MCC:CMC-Na		Particle size(nm) <sup>a</sup>	Particle size (nm) <sup>b</sup>	Zeta potential(mV)	RDI
N1	100:0	619.5 ± 15.2	1319.51 ± 24.1	-4.8 ± 0.3	2.1 ± 0.3
N2	95:5	349.7 ± 8.7	1249.7 ± 27.6	-20.1 ± 0.5	3.6 ± 0.2
N3	90:10	324.0 ± 7.9	824.3 ± 15.1	-35.2 ± 0.6	2.5 ± 0.3
N4	85:15	253.6 ± 11.5	356.2 ± 14.3	-42.1 ± 0.7	1.4 ± 0.2
N5	80:20	124.2 ± 2.5	163.5 ± 3.6	-45.8 ± 0.6	1.3 ± 0.1
N6	75:25	211.3 ± 7.1	233.7 ± 12.4	-55.3 ± 0.5	1.1 ± 0.1

<sup>a</sup> Represents the mean particle size of freshly prepared CNCC.

<sup>b</sup> Represents the mean particle size of spray-dried CNCC after reconstitution as Method 2.5.5.

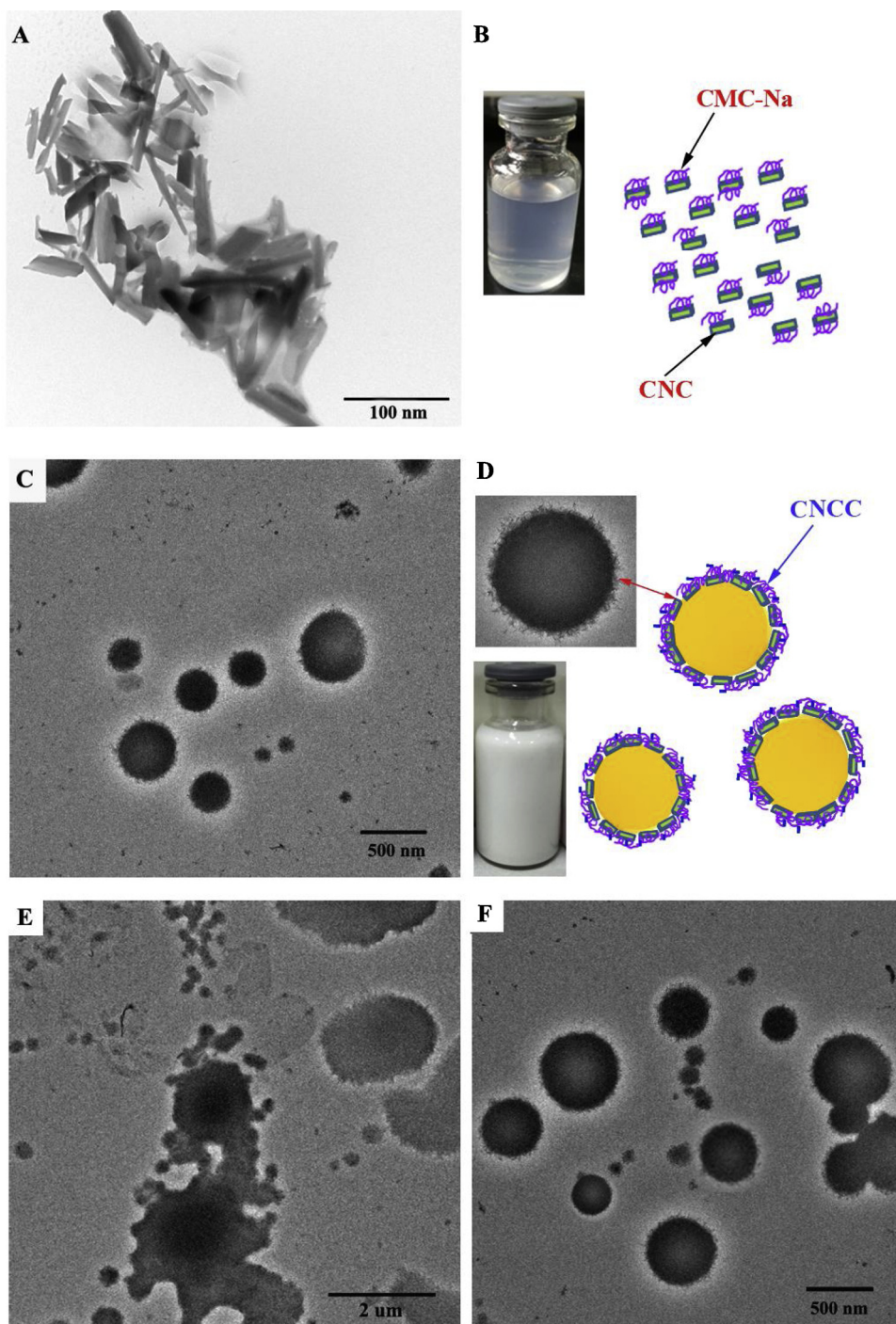


**Fig. 2.** TEM images of CNCC (A) and CO-PE/CNCC (C), and schematic images on formation mechanism of CNCC (B) and CO-PE/CNCC (D), and TEM images of the redispersed CO-PE/CNCC (E) and CO-PE/CNCC/HPMC (F).

(N1). The mean particle size ( $124.2 \pm 2.5$  nm) of CNCC modified with 20% CMC-Na (N5) was smallest of all the samples. This indicated that presence of CMC-Na could improve the particle-reduction efficiency of CNC during homogenization. It might be the reason that, CMC-Na could adsorb onto surface of CNC and decrease the surface energy of new generated CNC during homogenization owing to the wettability of CMC-Na (Yue et al., 2013). The morphology of CNCC modified with 20% CMC-Na (N5) was shown in the Fig. 2A. The CNCC appeared to be irregular rod-shaped particles. This was different from the ribbon-like morphology of the sulfuric acid hydrolysed CNC or TEMPO catalysed CNC (Helbert & Sugiyama, 1998; Camarero Espinosa, Kuhnt, Foster, & Weder, 2013). The treatment of high pressure homogenization could yield nano-scale cellulose particles with different morphology, which was consistent with earlier observations for a similarly produced material (Bandera et al., 2014; Buffiere et al., 2017). Furthermore, this might also be related with modification of CMC-Na during homogenization. As illustrated in Fig. 2B, this could be attributed to the electrostatic repulsion and steric barrier effect of CMC-Na adsorbed onto surface of CNC. The Zeta potential of CNCC was showed in Table 1. The results showed that the Zeta potential ( $-20.1$  to  $-55.3$  mV) of different CNCC was significantly less than that of CNC ( $-4.8$  mV), which could be attributed to the anionic polymer CMC-Na (Chittasupho, Thongnopkoon, & Kewsuwan, 2016). And the Zeta potential of CNCC was decreased with the increased concentrations of CMC-Na.

As shown in Table 1, the mean particle sizes of redispersed CNCC (N1~N6) after spray-drying were  $163.5 \pm 3.6$ – $1319.51 \pm 24.1$  nm. The results shown that, the particle size ( $1319.51 \pm 24.1$  nm) of redispersed CNC (N1) without CMC-Na was remarkably increased ( $p < 0.05$ ), compared with that of freshly prepared CNC ( $619.5 \pm 15.2$  nm). But the RDI (3.6–1.1) of spray-dried CNCC (N2~N6) was improved as the increased ratio of CMC-Na. And the RDI ( $1.3 \pm 0.1$ ) of dried CNCC modified with 20% CMC-Na (N5) was less than 1.5, which meant that CNCC(N5) could completely reconstitute into the original CNCC after rehydration (Yue et al., 2013; Zhang, Guan, Ni, Li, & Maom, 2014). It could be the reason that CMC-Na could adsorb onto the surface of CNC in order to prevent CNC from irreversible aggregations during spray-drying, and effectively enhanced the redispersion of CNC triggered by its swelling ability and aqueous solubility (Chen, Ho, Liu, Siow, & Sheu, 2015).

### 3.2. Characterization of solid state of CNCC

#### 3.2.1. XRD

Fig. 3 displayed the XRD diffractograms of raw MCC, CMC-Na, CNCC, and the mixture of MCC and CMC-Na. Raw MCC exhibited the characteristic peaks at  $2\theta$  of 16.4, 22.5 and 35.6° (Fig. 3A). This was consistent with the previous report (Wen et al., 2014). CMC-Na exhibited the characteristic peaks at  $2\theta$  of 21.7° (Fig. 3B). The physical mixture of MCC and CMC-Na exhibited the similar characteristic peaks of MCC and CMC-Na (Fig. 3C). Furthermore, CNCC had similar crystalline characteristic peaks (Fig. 3D), compared with the mixture of MCC and CMC-Na. There still existed the characteristic peak of MCC and CMC-Na at the same  $2\theta$  position demonstrating that the crystal state of CNCC was not changed during homogenization.

#### 3.2.2. Spectrum of IR

The infrared spectra of MCC, CMC-Na, mixture of MCC and CMC-Na, and the CNCC powder were shown in Fig. 4. Fig. 4A showed the characteristic absorption peak of MCC: OH,  $3345$   $\text{cm}^{-1}$ ; C–H,  $2850$   $\text{cm}^{-1}$ ; C–O–C–O–C,  $1033$ – $1113$   $\text{cm}^{-1}$ . Fig. 4B showed that characteristic absorption peaks of CMC-Na: OH,  $3440$   $\text{cm}^{-1}$ ; C–H,  $2972$   $\text{cm}^{-1}$ ; C=O,  $1595$   $\text{cm}^{-1}$ . The spectrum of the mixture of MCC and CMC-Na (Fig. 4C) was similar with that of the MCC, and the signals at  $3345$   $\text{cm}^{-1}$ ;  $2890$   $\text{cm}^{-1}$ ;  $1638$   $\text{cm}^{-1}$  and  $1033$ – $1113$   $\text{cm}^{-1}$  indicated that the presence of cellulose structure, but the peaks of CMC-Na at

$3440$   $\text{cm}^{-1}$ ; and C=O,  $1595$   $\text{cm}^{-1}$  were almost superimposable upon that of MCC. The adsorption spectrum of the mixture of MCC and CMC-Na showed a combination effect of MCC and CMC-Na. And there was no significant difference between the mixture (Fig. 4C) and the spray-dried CNCC powder (Fig. 4D). These results demonstrated the characteristics peaks of MCC were still visible in the spray-dried CNCC. Moreover, no new peaks were observed in CNCC, indicating no significant changes of the cellulose structure of CNCC. It might be the reason that the combination of CNC and CMC-Na in the spray-dried CNCC might be dependent of physical interaction, attributed to formation of Vander Waals forces or hydrogen bond (Behra, Giri, Tripathi, & Ajazuddin, 2012; Zhao, Kapur, Carlin, Selinger, & Guthrie, 2011; Behra et al., 2012).

#### 3.2.3. DTG and DSC

Thermal decomposition parameters were determined from DTG curves as described below at a heating rate of  $5$   $^{\circ}\text{C}\cdot\text{min}^{-1}$ . The DTG curves of MCC, CMC-Na, the mixture of MCC and CMC-Na, CNCC powder were shown in Fig. 5. The DTG curve of MCC and CMC-Na respectively showed a main peak at  $300$  and  $280$   $^{\circ}\text{C}$ , which accounted for the endothermic peak for pyrolysis of MCC and CMC-Na (Wen et al., 2014). The thermal degradation of CNCC powder showed the similar decomposition peak of MCC and CMC-Na. But the thermal degradation of CNCC started at a much lower temperature ( $\approx 225$   $^{\circ}\text{C}$ ) as compared to all other samples. It might be the reason that particles size reduction and/or crystals defect of CNCC subjected to homogenization (Dan et al., 2016; Li et al., 2018).

Fig. 6 showed that thermal behavior of raw MCC and CNCC between  $30$   $^{\circ}\text{C}$  and  $300$   $^{\circ}\text{C}$ . It could be seen that MCC showed wide endothermic peak in the investigated range, which might be attributed to hierarchical organization (crystalline and amorphous fractions) of MCC (George & Sabapathi, 2015; Buffiere et al., 2017). CNCC exhibited similar thermal behavior in comparison to that of MCC, but the enthalpy of CNCC was decreased, which was possibly attributed to particles size reduction of CNCC. The enthalpy of melting for a nanocrystal decrease as its size decrease based on the Mott's equation (Zhang, Lu, & Jiang, 1999; Singh, Lara, & Tlali, 2017).

### 3.3. Influencing of different concentrations of CNCC on formulation of CO-PE/CNCC and CO-PEP/CNCC

The particles size (D10, D50 and D90) of freshly prepared CO-PE/CNCC stabilized by different concentrations of CNCC were showed in Fig. 7. The results showed that the D50 and D90 of freshly prepared CO-PE/0.05%CNCC was  $1.946$  and  $2.862$   $\mu\text{m}$ , respectively. Due to its large particles size, CO-PE/0.05%CNCC was liable to coalescence and/or agglomeration. This meant that the 0.05% CNCC was not able to effectively stabilize Pickering emulsion. It could be also seen that, the particle size (D50) of CO-PE/0.1%CNCC was remarkably decreased ( $p < 0.05$ ), compared with that of N1. And the mean particle size of CO-PE/0.25%CNCC was  $0.569 \pm 0.023$   $\mu\text{m}$ . But the particle size of CO-PE with higher concentrations of CNCC (from 0.5% to 1%) seemed to be larger in comparison to CO-PE/0.25%CNCC. Therefore, the mean particle size of CO-PE/0.25%CNCC was smallest among all the formulations. And the TEM image of CO-PE/0.25%CNCC was showed in Fig. 2C. It could be seen that the morphology of CO-PE/0.25%CNCC was intact sphere-shaped droplets. This seemed to be different from the collapsed structures of conventional Pickering emulsion droplets. As illustrated in Fig. 2D, it could be speculated that, this CNCC based particle stabilizer could adsorb onto the surface of oil droplet and form the distinctive steric barrier shell, and CMC-Na might enhance the strength of steric barrier of CNCC and filled up the collapsed structures of emulsion droplets (Zhen et al., 2016). And this steric barrier effect of CNCC could effectively maintain the stability of CO-PE.

Fig. 7 also showed that, the particles size of redispersed CO-PE/CNCC after spray-drying was remarkably increased ( $p < 0.05$ ),

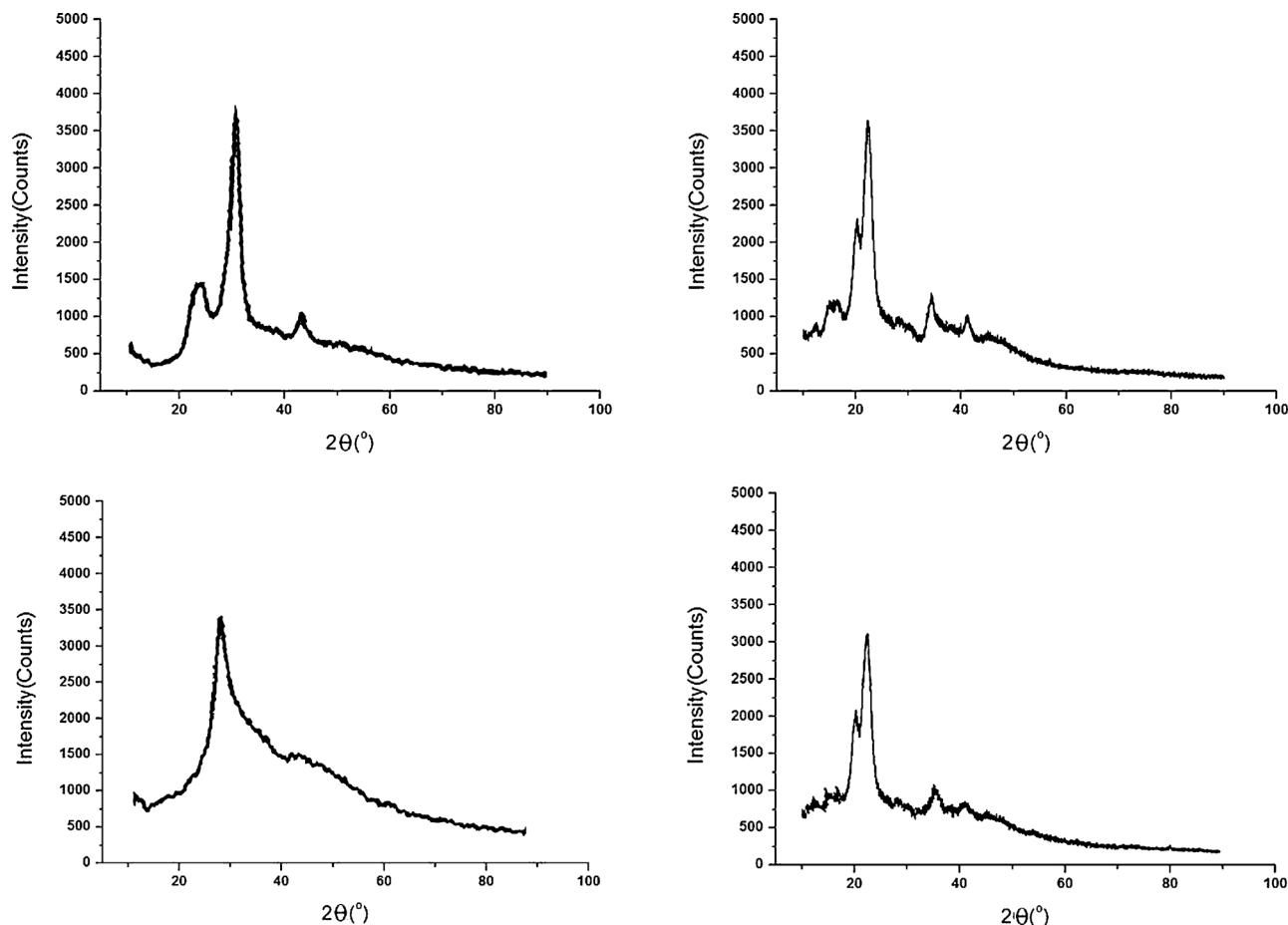


Fig. 3. XRD diffractograms of raw MCC (A), CMC-Na (B), the mixture of MCC and CMC-Na(C), and CNCC(D).

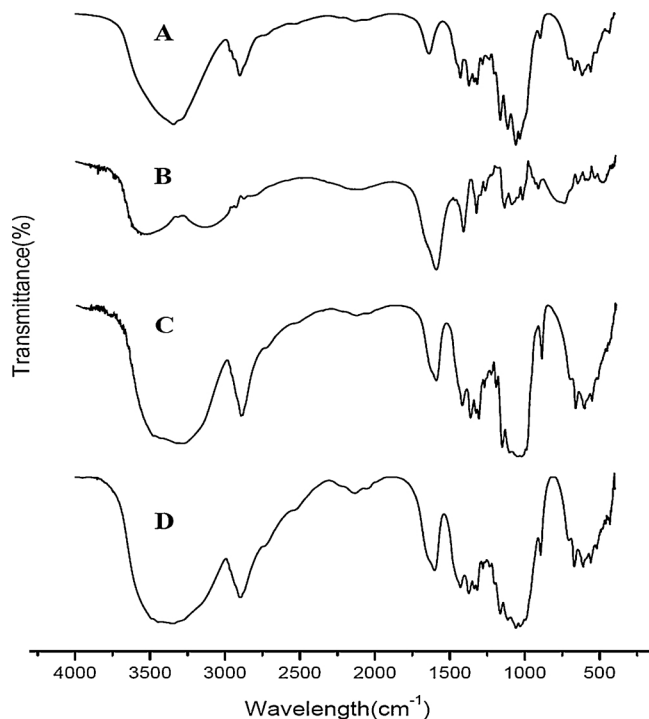


Fig. 4. The IR spectrum of MCC (A), CMC-Na (B), the mixture of MCC and CMC-Na (C), CNCC (D).

compared with particle size of freshly prepared CO-PE/CNCC. The RDIs of spray-dried CO-PEP/CNCC were more than 1.5, which meant that it had occurred agglomeration of the emulsion droplets during spray-drying (Xie et al., 2019; Zhang et al., 2014). And the Fig. 2E also showed the presence of some large coalescence and/or growth droplet in the redispersed CO-PE/0.25%CNCC. Therefore, in order to prevent coalescence of the emulsion droplets and/or oil leakage, hydrophilic matrix formers, including lactose, trehalose, inulin, maltodextrin and hydroxypropyl methylcellulose (HPMC), should be added into the CO-PE/CNCC formulations after emulsification, and further evaluated as follows.

### 3.4. Influencing of different matrix formers on redispersibility of spray-dried CO-PEP/CNCC

Fig. 8 showed that the RDIs of spray-dried CO-PEP/0.25%CNCC with different matrix formers. The results demonstrated that using CNCC as matrix formers, the RDI of CO-PEP was more than 2, even though using 200% concentration (relative to the weight of oil phase, w/w). This meant that CNCC could not effectively prevent coalescence of emulsions droplet during spray-drying (Yue et al., 2013; Zhang et al., 2014).

RDI of CO-PEP/CNCC respectively using 200% concentration (relative to the weight of oil phase, w/w) of lactose, trehalose, inulin and maltodextrin as matrix formers was more nearer to 1, compared to those of 50% and 100% concentrations. And RDI of PEP/CNCC respectively using 100% concentration of CMC-Na and arabic gum as matrix formers was less than 1.5. However, RDI of CO-PEP/0.25%CNCC/50%HPMC was  $1.12 \pm 0.09$ , and Fig. 2F showed that the morphology of redispersed CO-PEP/0.25%CNCC/50%HPMC seemed to

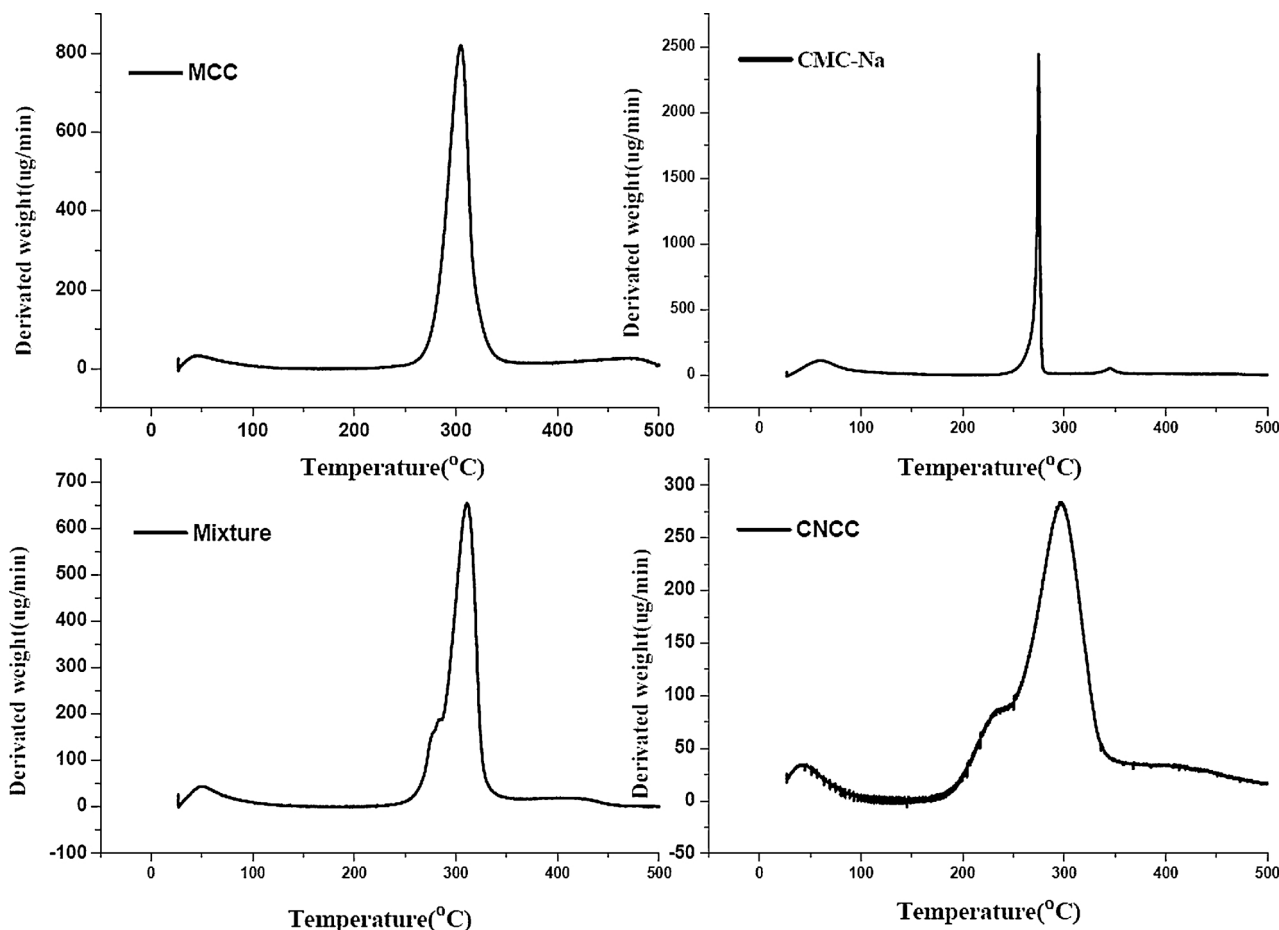


Fig. 5. The DTG of MCC, CMC-Na, mixture of MCC and CMC-Na, and CNCC.

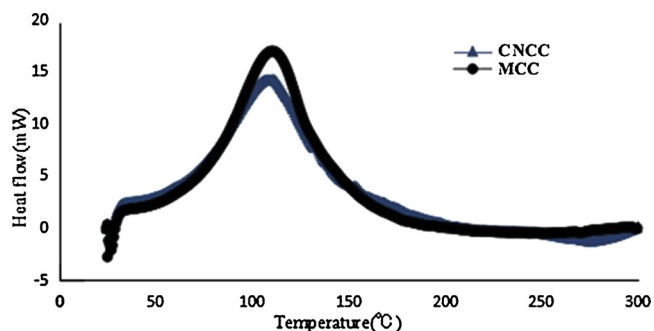


Fig. 6. The analysis thermograms of DSC of MCC and CNCC.

be sphere-shaped droplets with particle size of 600 nm, which was consistent with the morphology of original CO-PE/0.25%CNCC (Fig. 2C). This indicated CO-PEP/0.25%CNCC/50%HPMC could reconstitute into the original CO-PE after rehydration. It was concluded that the types and concentrations of matrix formers played an important role in maintaining the redispersibility of CO-PEP. And the higher the concentration of matrix formers was, the better protection of matrix formers was at three concentrations. Furthermore, 50% HPMC, 100% maltodextrin, CMC-Na, arabic gum could effectively protected CO-PEP from droplet coalescence during spray-drying, respectively. It could be also seen that of all the matrix formers, the redispersibility of HPMC based CO-PEP was relatively superior.

### 3.5. Morphology of CO-PEP/CNCC

The morphology results of optimum spray-dried CO-PEP was showed in Fig. 9 A–D. The results showed no evidence of cracking in the particles produced using the optimum matrix formers, which was important to prevent leakage of oil. It also showed that the 100% maltodextrin based CO-PEP/CNCC exhibited smaller particle size in comparison to the other matrix formers (HPMC, CMC-Na or arabic gum) based CO-PEP. But maltodextrin based CO-PEP could form more hygroscopic particles, which was evidenced by the formation of solid bridges and fusion of small particles (Fig. 9A). This could be due to the easily hygroscopic property of maltodextrin, which resulted in the adhesion property (stickiness) of particles during spray-drying (Jang et al., 2006). Interestingly, the surface of the CO-PEP/CNCC particles appeared to be wrinkled. This wrinkled-surface might be related with a collapsed coating shell which was initially inflated during drying process owing to the internal vapour formation (Sou et al., 2016). But the CO-PEP containing maltodextrin exhibited a higher proportion of spherical particles, most likely because maltodextrin provided relatively lower viscosity during the drying process (Jafari, Assadpoor, He, & Bhandari, 2008; Fernandes et al., 2014). The CO-PEP particles using HPMC, CMC-Na, arabic gum as matrix formers (Fig. 9B–D) possessed greater surface corrugations, respectively compared to the CO-PEP/CNCC containing maltodextrin. Therefore, the presence of water soluble polymers could also affect the surface morphology of CO-PEP/CNCC. Furthermore, CO-PEP/HPMC exhibited larger particle size compared with other CO-PEP/CNCC containing other matrix formers. It might be the reason that HPMC was reported as film-forming agents which could form particles with wrinkled or dimpled morphology after spray-drying (Vehring, 2008). But the combination of CNCC and HPMC

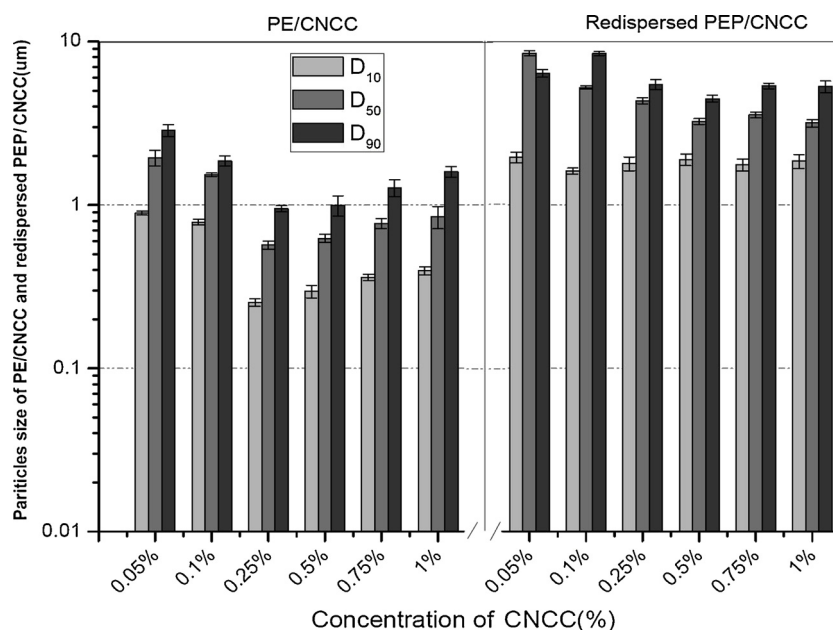


Fig. 7. Particle size of CO-PE/CNCC and redispersed CO-PE/CNCC(μm).

might have a synergistic effect on formation of CO-PEP, which might result in an increased loading efficiency.

#### 4. Conclusions

The novel Pickering emulsions stabilizer by CNCC modified with CMC-Na as particle stabilizer was successfully prepared by homogenization technology, and further converted into redispersible Pickering emulsions powder using HPMC as matrix former. CNCC particles modified with CMC-Na were firstly prepared by homogenization technology. The characterization evaluations demonstrated that the cellulose structure and crystal state of CNC in CNCC remained unchanged during the homogenization. The combination of CNC and CMC-Na in CNCC might be dependent of physical interaction. CO-PE stabilized by CNCC was successfully prepared, which might be attributed to the CNCC based steric barrier. Furthermore, optimum HPMC based CO-PEP/CNCC could completely prevent from aggregation of

droplets during spray-drying and enhance the redispersibility of CO-PEP. This study demonstrated that novel redispersible powdered Pickering emulsions could be prepared by cellulose nanocrystals coupling with water-soluble cellulosic derivatives. This also would provide a feasible strategy for encapsulation of oil soluble drug.

#### Disclosure

The authors report no conflicts of interest in this work.

#### Acknowledgments

The authors would like to acknowledge the financial support from the Scientific Research Foundation for the National Natural Science Foundation of China (81760715), the Young Jinggang Scholar Award Program and Fund of Distinguished Young Scientists of Jiangxi Province (20162BCB23033).

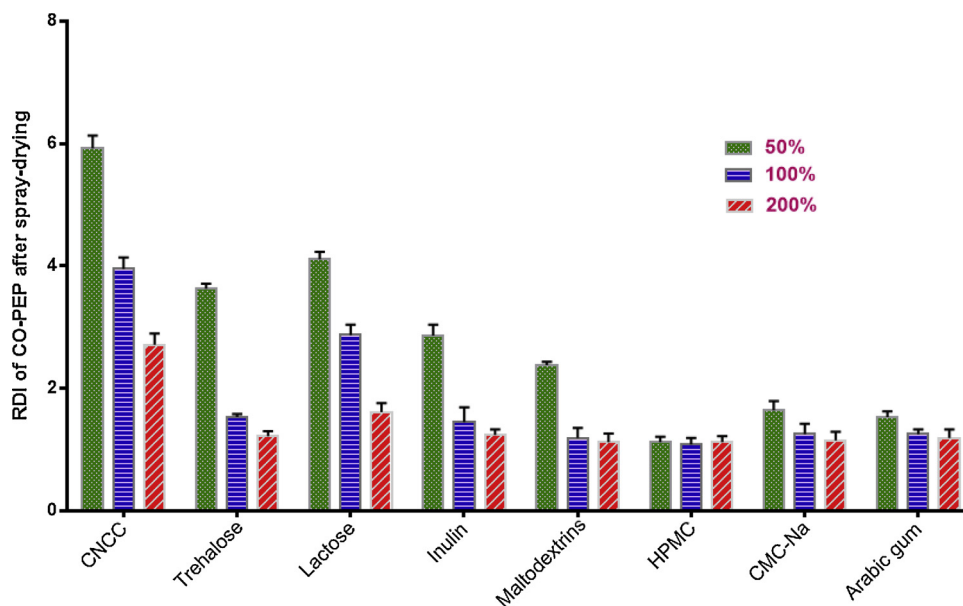
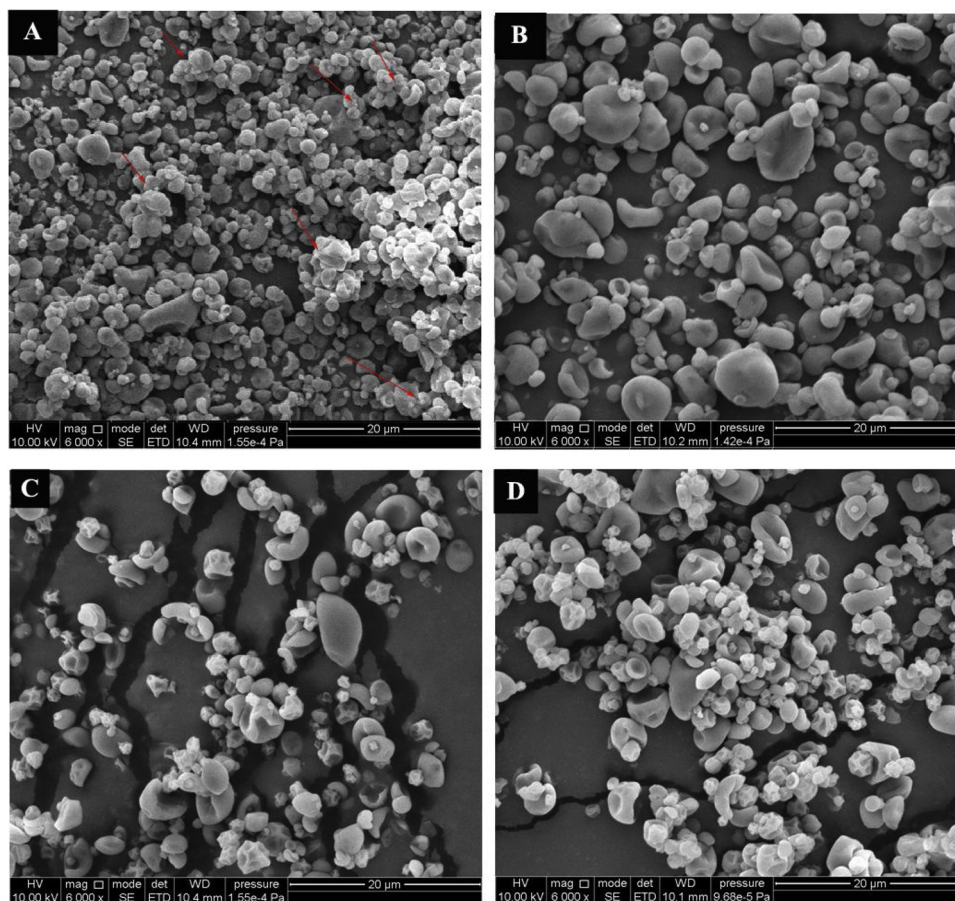


Fig. 8. RDI of spray-dried CO-PEP/CNCC containing different matrix formers.



**Fig. 9.** SEM images of CO-PEP/CNCC/100% maltodextrin (A), CO-PEP/CNCC/50%HPMC (B), CO-PEP/CNCC/100% CMC-Na(C), and CO-PEP/CNCC/100% arabic gum(D).

## References

- Asensio, C. M., Paredes, A. J., Martin, M. P., Allemandi, D. A., Nepote, V., & Grosso, N. R. (2017). Antioxidant stability study of oregano essential oil microcapsules prepared by spray-drying. *Journal of Food Science*, *82*(12), 2864–2872.
- Bandera, D., Sapkota, J., Josset, S., Weder, C., Tingaut, P., Gao, X., et al. (2014). Influence of mechanical treatments on the properties of cellulose nanofibers isolated from microcrystalline cellulose. *Reactive & Functional Polymers*, *85*, 134–141.
- Basha, M., Salama, A. H., & El Awdan, S. (2017). Reconstitutable spray-dried ultra-fine dispersion as a robust platform for effective oral delivery of an antihyperlipidemic drug. *International Journal of Pharmaceutics*, *532*(1), 478–490.
- Behra, A., Giri, T. K., Tripathi, D. K., & Ajazuddin, A. A. (2012). An exhaustive review on recent advancement in pharmaceutical bioadhesive used for systemic drug delivery through oral mucosa for achieving maximum pharmacological response and effect. *International Journal of Pharmacology*, *8*, 283–305.
- Berton-Carabin, C. C., & Schroën, K. (2015). Pickering emulsions for food applications: Background, trends, and challenges. *Annual Review of Food Science and Technology*, *6*, 263–297.
- Buffiere, J., Balogh-Michels, Z., Borrega, M., Geiger, T., Zimmermann, T., & Sixta, H. (2017). The chemical-free production of nanocelluloses from microcrystalline cellulose and their use as Pickering emulsion stabilizer. *Carbohydrate Polymers*, *178*, 48–56.
- Camarero Espinosa, S., Kuhnt, T., Foster, E. J., & Weder, C. (2013). Isolation of thermally stable cellulose nanocrystals by phosphoric acid hydrolysis. *Biomacromolecules*, *14*(4), 1223–1230.
- Chen, Y. C., Ho, H. O., Liu, D. Z., Siow, W. S., & Sheu, M. T. (2015). Swelling/floatability and drug release characterizations of gastroretentive drug delivery system based on a combination of hydroxyethyl cellulose and sodium carboxymethyl cellulose. *PLoS One*, *10*(1), e0116914.
- Chittasupho, C., Thongnopkoon, T., & Kewsuwan, P. (2016). Surface modification of poly (D,L-lactic-co-glycolic acid) nanoparticles using sodium carboxymethyl cellulose as colloidal stabilizer. *Current Drug Delivery*, *13*(1), 95–104.
- Christensen, K. L., Pedersen, G. P., & Kristensen, H. G. (2001). Preparation of redispersible dry emulsions by spray drying. *International Journal of Pharmaceutics*, *212*(2), 187–194.
- Da Costa, J. M., Borges, S. V., Hijo, A. A., Silva, E. K., Marques, G. R., Cirillo, M. Á., et al. (2013). Matrix structure selection in the microparticles of essential oil oregano produced by spray dryer. *Journal of Microencapsulation*, *30*(8), 717–727.
- Dan, J., Ma, Y., Yue, P., Xie, Y., Zheng, Q., Hu, P., et al. (2016). Microcrystalline cellulose-carboxymethyl cellulose sodium as an effective dispersant for drug nanocrystals: A case study. *Carbohydrate Polymers*, *2016*(136), 499–506.
- Dollo, G., Le Corre, P., Guérin, A., Chevanne, F., Burgot, J. L., & Leverage, R. (2013). Spray-dried redispersible oil-in-water emulsion to improve oral bioavailability of poorly soluble drugs. *European Journal of Pharmaceutical Sciences : Official Journal of the European Federation for Pharmaceutical Sciences*, *19*(4), 273–280.
- Fernandes, R. V., Borges, S. V., & Botrel, D. A. (2014). Gum arabic/starch/maltodextrin/inulin as wall materials on the microencapsulation of rosemary essential oil. *Carbohydrate Polymers*, *101*, 524–532.
- Fujisawa, S., Togawa, E., & Kuroda, K. (2017). Nanocellulose-stabilized Pickering emulsions and their applications. *Science and Technology of Advanced Materials*, *18*(1), 959–971.
- George, J., & Sabapathi, S. N. (2015). Cellulose nanocrystals: Synthesis, functional properties, and applications. *Nanotechnology, Science and Applications*, *8*, 45–54.
- Goula, A. M., & Adamopoulos, K. G. (2008). Effect of maltodextrin addition during spray drying of tomato pulp in dehumidified air: I. Powder properties. *Drying Technology*, *26*, 726–737.
- Habibi, Y., Lucia, L. A., & Rojas, O. J. (2010). Cellulose nanocrystals: Chemistry, self-assembly, and applications. *Chemical Reviews*, *110*(6), 3479–3500.
- Helbert, W., & Sugiyama, J. (1998). High-resolution electron microscopy on cellulose II and  $\alpha$ -chitin single crystals. *Cellulose*, *5*, 113–122.
- Hu, Z., Patten, T., Pelton, R., & Cranston, E. D. (2015). Synergistic stabilization of emulsions with cellulose nanocrystals and cellulose derivatives. *ACS Sustainable Chemistry & Engineering*, *3*(5), 1023–1031.
- Hu, Z., Marway, H. S., Kasem, H., Pelton, R., & Cranston, E. D. (2016). Dried and redispersible cellulose nanocrystal Pickering emulsions. *ACS Macro Letters*, *5*(2), 185–189.
- Jafari, S. M., Assadpoor, E., He, Y., & Bhandari, B. (2008). Encapsulation efficiency of food flavours and oils during spray drying. *Drying Technology*, *26*, 816–835.
- Jang, D. J., Jeong, E. J., Lee, H. M., Kim, B. C., Lim, S. J., & Kim, C. K. (2006). Improvement of bioavailability and photostability of amlodipine using redispersible dry emulsion. *European Journal of Pharmaceutical Sciences : Official Journal of the European Federation for Pharmaceutical Sciences*, *28*(5), 405–411.
- Kalashnikova, I., Bizot, H., Cathala, B., & Capron, I. (2011). Modulation of cellulose nanocrystals amphiphilic properties to stabilize oil/water interface. *Biomacromolecules*, *13*(1), 267–275.
- Li, X., Li, J., Gong, J., Kuang, Y., Mo, L., & Song, T. (2018). Cellulose nanocrystals (CNCs) with different crystalline allomorph for oil in water Pickering emulsions.

- Carbohydrate Polymers*, 183, 303–310.
- Liu, Y., Xiao, H., Xie, J., Zhang, Z., Ma, Y., Yue, P., et al. (2018). The shielding effect of microcrystalline cellulose on drug nanocrystal particles during compaction. *AAPS PharmSciTech*, 19(6), 2488–2498.
- Ma, Y., Yang, Y., Xie, J., Xu, J., Yue, P., & Yang, M. (2018). Novel nanocrystal-based solid dispersion with high drug loading, enhanced dissolution, and bioavailability of andrographolide. *International Journal of Nanomedicine*, 13, 3763–3779.
- Mao, L., Roos, Y. H., Biliaderis, C. G., & Miao, S. (2017). Food emulsions as delivery systems for flavor compounds: A review. *Critical Reviews in Food Science and Nutrition*, 57(15), 3173–3187.
- Marto, J., Ascenso, A., Simoes, S., Almeida, A. J., & Ribeiro, H. M. (2016). Pickering emulsions: Challenges and opportunities in topical delivery. *Expert Opinion on Drug Delivery*, 13(8), 1093–1107.
- Natterodt, J. C., Sapkota, J., Foster, E. J., & Weder, C. (2017). Polymer nanocomposites with cellulose nanocrystals featuring adaptive surface groups. *Biomacromolecules*, 18(2), 517–525.
- Singh, M., Lara, S., & Tlali, S. (2017). Effects of size and shape on the specific heat, melting entropy and enthalpy of nanomaterials. *Journal of Taibah University for Science : JTUSCI*, 11(6), 922–929.
- Sou, T., Forbes, R. T., Gray, J., Prankerd, R. J., Kaminskas, L. M., McIntosh, M. P., et al. (2016). Designing a multi-component spray-dried formulation platform for pulmonary delivery of biopharmaceuticals: The use of polyol, disaccharide, polysaccharide and synthetic polymer to modify solid-state properties for glassy stabilization. *Powder Technology*, 287, 248–255.
- Sunasee, R., Hemraz, U. D., & Ckless, K. (2016). Cellulose nanocrystals: A versatile nanoplatform for emerging biomedical applications. *Expert Opinion on Drug Delivery*, 13(9), 1243–1256.
- Vehring, R. (2008). Pharmaceutical particle engineering via spray drying. *Pharmaceutical Research*, 25, 999–1022.
- Wang, Y., Zheng, Y., Zhang, L., Wang, Q., & Zhang, D. (2013). Stability of nanosuspensions in drug delivery. *Journal of Controlled Release : Official Journal of the Controlled Release Society*, 28(3), 1126–1141 172.
- Wen, C., Yuan, Q., Liang, H., & Vriesekoop, F. (2014). Preparation and stabilization of D-limonene Pickering emulsions by cellulose nanocrystals. *Carbohydrate Polymers*, 112, 695–700.
- Wu, J., & Ma, G. H. (2016). Recent studies of Pickering emulsions: Particles make the difference. *Small*, 12(34), 4633–4648.
- Xie, J., Luo, Y., Liu, Y., Ma, Y., Yue, P., & Yang, M. (2019). Novel redispersible nanosuspensions stabilized by co-processed nanocrystalline cellulose-sodium carboxymethyl starch for enhancing dissolution and oral bioavailability of baicalin. *International Journal of Nanomedicine*, 14, 353–369.
- Yang, X., Bakaic, E., Hoare, T., & Cranston, E. D. (2013). Injectable polysaccharide hydrogels reinforced with cellulose nanocrystals: Morphology, rheology, degradation, and cytotoxicity. *Biomacromolecules*, 14, 4447–4455.
- Yang, Y., Fang, Z., Chen, X., Zhang, W., Xie, Y., Chen, Y., et al. (2017). An overview of Pickering emulsions: Solid-Particle materials, classification, morphology, and applications. *Frontiers in Pharmacology*, 8, 287–307.
- Yue, P., Li, Y., Wan, J., Yang, M., Zhu, W., & Wang, C. (2013). Study on formability of solid nanosuspensions during nanodispersion and solidification: I. Novel role of stabilizer/drug property. *International Journal of Pharmaceutics*, 454(1), 269–277.
- Zhang, X., Guan, J., Ni, R., Li, L., & Maom, S. (2014). Preparation and solidification of redispersible nanosuspensions. *Journal of Pharmaceutical Sciences*, 103(7), 2166–2176.
- Zhang, Z., Lu, X. X., & Jiang, Q. (1999). Finite size effect on melting enthalpy and melting entropy of nanocrystals. *Physica B*, 270, 249–254.
- Zhao, G. H., Kapur, N., Carlin, B., Selinger, E., & Guthrie, J. T. (2011). Characterisation of the interactive properties of microcrystalline cellulose-carboxymethyl cellulose hydrogels. *International Journal of Pharmaceutics*, 415(1-2), 95–101.
- Zhou, Y., Sun, S., Bei, W., Zahi, M. R., Yuan, Q., & Liang, H. (2018). Preparation and antimicrobial activity of oregano essential oil Pickering emulsion stabilized by cellulose nanocrystals. *International Journal of Biological Macromolecules*, 112, 7–13.